Adsorption of Water on TiC(100): Evidence for Complex Reaction and Desorption Pathways

Philip B. Merrill[†] **and Scott S. Perry***

Department of Chemistry, University of Houston, Houston, Texas 77204-5641

Peter Frantz and Stephen V. Didziulis

Surface Science Department, Mechanics and Materials Technology Center, The Aerospace Corporation, El Segundo, California 90245

Received: April 24, 1998; In Final Form: July 15, 1998

The interaction of water with the nonpolar TiC(100) face has been probed as a function of surface temperature over the range 98−773 K. Temperature-programmed desorption (TPD) has been used to monitor the desorption products as a function of coverage while high-resolution electron energy loss spectroscopy (HREELS) has been used to probe the nature of adsorbed species as a function of surface temperature. Together, these molecularly specific probes reveal the presence of both molecularly and dissociatively adsorbed water in the monolayer regime at cryogenic temperatures. Furthermore, both Ti and C surface atoms participate in the dissociation of water and lead to the production of a complex array of surface species. With increasing surface temperature, the desorption species D_2O, CO, CO_2, and D_2 are observed over a broad temperature range. The desorption of CO and CO_2 demonstrates the consumption of carbon from the TiC surface while the desorption of D_2 is thought to be related to presence of carbon vacancies known to exist within this and other metal carbides.

Introduction

Compound materials such as metal carbides are becoming increasingly important in applications that require tailored chemical, physical, and mechanical properties. Coatings technology represents such an application. Here, a thin layer of a material, designed to perform a specific function, is deposited on top of a supporting substrate that is usually macroscopic in comparison to the coating thickness. In the past, coatings have been designed to enhance optical properties, to modify or passivate chemical reactivity, or to improve tribological properties. In tribological applications, the chemical reactivity, interfacial hardness, and frictional properties of the compound material all contribute to the performance of the coating.

Transition metal carbides and nitrides are currently employed as tribological coatings in bearing systems and cutting tools.[1,2] These materials have initially been chosen for their high hardness,[3] a property desirable for reducing the interfacial wear of the mechanical part that is being coated. While reductions in wear have been realized, a complete understanding of the chemical and frictional properties of these materials is needed to provide a complete design of the tribological interface.

Initial studies of the chemical properties of compound surfaces such as metal carbides and nitrides have indicated that unique reactivities are observed with respect to the parent metal.[4−7] For the metal atoms, such a change is not surprising as the bulk electronic structure and local bonding at the surface are distinctly different from that of the transition metal surface.[7−9] In addition to this perturbation to the surface, nonmetal atoms are present, again with unique electronic and structural properties, and can contribute to the surface chemistry. There thus exists the possibility of novel channels of surface reactivity and thereby warrants the study of compound surfaces from a fundamental point of view.

In this study, we have investigated the chemical reactivity of single-crystal titanium carbide (TiC) with water, a small molecule of immense tribological importance. The nonpolar (100) face of this rock-salt material, which presents equal numbers of metal and nonmetal atoms, can be considered the simplest of the different faces of this compound material and has been chosen as a fundamental starting point to the study of the surface chemistry of titanium carbide. We have used temperature-programmed desorption (TPD) and high-resolution electron energy loss spectroscopy (HREELS) to investigate the chemical reactivity of this TiC surface with water. We find that TPD reveals several different desorption and reaction pathways of water while HREELS reveals the presence of both molecularly and dissociatively adsorbed water on TiC(100). By performing HREELS experiments as a function of surface temperature, we are able to generate a molecularly specific picture of the adsorption, reaction, and desorption for this system. The nature of these surface-mediated processes will be discussed in terms of both the composition of surface species and the products of the desorption process.

Experimental Section

The TiC(100) single crystal used in the TPD study was obtained as a gift from UBE Industries of Japan. The method of growth has been described in the literature.[10] The crystal was polished with diamond paste down to 0.05 μm finish and cleaned with acetone and ethanol. X-ray photoelectron spec-

* Corresponding author: e-mail perry@uh.edu; FAX (713) 743-2709.
[†] Present address: Evans Texas, 425 Round Rock West Drive, Suite 100, Round Rock, TX 78681.

S1089-5647(98)01982-8 CCC: $15.00
Published on Web 09/09/1998

troscopy (XPS) results show the surface to have a 1:1 stoichiometry (±5%).[8] Argon (Matheson, prepurified, 99.998%) gas was used for sputter cleaning without further purification. Freeze/pump/thaw cycles were used to eliminate dissolved gases from the D_2O (Aldrich, 99.96 atom % D) prior to use.

Thermal desorption experiments have been performed in a stainless steel ultrahigh-vacuum (UHV) chamber with a base pressure of 2×10^{-10} Torr. This system, which has been previously described in greater detail,[11] is equipped with a retarding field analyzer (Omicron Instruments) for low-energy electron diffraction (LEED) and Auger electron spectroscopy (AES), an ion gun (Omicron Instruments) for argon bombardment, and a quadrupole mass spectrometer (Fisons/V.G. Quartz 200) for temperature-programmed desorption (TPD). The chamber also houses a scanning probe microscope capable of operating as either a scanning tunneling microscope (STM) or an atomic force microscope (AFM).

For the TPD measurements, the TiC(100) sample was mounted with strips of tantalum foil to a tantalum sample holder. When affixed to the sample manipulator (Thermionics Northwest Laboratories), thermal contact of this plate with a liquid nitrogen reservoir allowed cooling to 98 K, while an internal filament provided radiative heating to 1273 K. Higher temperatures were achieved by electron bombardment through biasing the sample plate at potentials up to 1 kV. Temperature measurement utilized a type K (chromel−alumel) thermocouple mounted on the sample face under the tantalum strips.

Unless otherwise noted, the TiC(100) surface was prepared by repeated cycles of room-temperature sputtering (1 kV) and anneals (5 min at 1500 K) until no impurities were detectable by AES. This surface exhibited a sharp (1×1) low-energy electron diffraction (LEED) pattern indicating excellent surface crystallographic order.[12]

In preparing samples for TPD measurements, the adsorption of gases has been limited to the crystal face through the use of a pinhole doser.[13,14] This doser consists of a 2 μm pinhole and a drift tube (5 mm i.d.) attached to a bellows. In vacuum, the sample face is positioned within 0.5 mm of the end of the tube, such that all gas effusing from the tube must strike the sample face. Gases to be adsorbed can be transferred into an isolated reservoir behind the orifice where pressure is monitored with a Convectron gauge. A fixed diffusion rate through the pinhole is achieved by holding a constant pressure on the gas handing side. Precise timing of the gas exposures and control of backing pressures provide excellent reproducibility of coverages.

After dosing the desired adsorbate, the sample was positioned toward the ionizer of the mass spectrometer at a distance of approximately 2 cm. A linear heating profile (temperature vs time) with a rate of 4 K/s was obtained over the relevant temperature ranges. The mass spectrometer signals were computer multiplexed to allow simultaneous detection of up to 15 masses as well as the sample temperature (via an isolation amplifier). The mass-to-charge ratios (m/q) monitored in these experiments were 2 (H_2^+,D^+), 4 (D_2^+), 18 (H_2O^+, OD^+), 20 (D_2O^+), 28 (CO^+), 32 (O_2^+), and 44 (CO_2^+). All data were collected using the same mass spectral sensitivities. In the following figures, an arbitrary y-offset has been utilized to display some of the multiple sets of data.

D_2O was utilized in all temperature-programmed desorption (TPD) experiments to differentiate desorption products from those arising from the adsorption of background quantities of H_2O present in the chamber. Background levels for deuterated species were significantly lower than water; consequently, the molecular ion ($m/q = 20$) as well as the reaction product D_2 ($m/q = 4$) could be attributed to the purposefully adsorbed D_2O species. In all cases, masses 18 and 2 were monitored simultaneously and showed identical desorption and reactivity, yet the desorption yields were minor (less than 5%).

High-resolution electron energy loss spectra (HREELS) were collected at The Aerospace Corporation with a double-pass spectrometer (LK 2000, LK Technologies, Inc.) with a beam current of 10^{-10} A, a resolution of 11 meV, and an elastic peak intensity of 3×10^5 counts/s. Spectra were collected digitally and typically took 1 h each. The angle of incidence of the electrons was fixed at 60° with respect to the surface normal, and the signal was collected along the specular direction. Spectra were obtained with incident beam energies of 7 eV, and the pass energy of the analyzer was 2 eV. The vacuum system housing the HREELS spectrometer has been described previously in greater detail.[15] A different TiC(100) sample was used for the HREELS studies; however, previous HREELS studies on the TiC sample used for TPD have indicated no structural or chemical differences between the two single-crystal samples.[12] The TiC(100) surfaces were prepared for these studies by methods analogous to the ones described above.

Gas exposures (D_2O, Aldrich, 99.96 atom % D; H_2O, Aldrich, HPLC grade) for the HREELS experiments were performed by placing the sample in the path of a gas dosing system that consisted of a turbo-pumped gas supply, a leak valve, and a 0.25 in. dosing tube terminated by a channel plate. This system has demonstrated an enhancement in direct dosing exposures of about 25 times relative to background exposures. Sample heating in this system was performed with a resistively heated tungsten filament mounted directly behind the sample stage on the manipulator. Cooling was provided through a copper braid attached to a liquid nitrogen cooled heat sink. The sample temperature was monitored through a type K thermocouple on the sample stage that was later calibrated with temperature measurements with the thermocouple directly located at the sample position (in analogy to the measurements at the University of Houston). The dosing temperature for the HREELS experiments was the lowest obtainable sample temperature (144 K) and was limited by the copper braid cooling design.

Results

Thermal Desorption of D_2O from TiC(100). The coverage-dependent desorption features of D_2O from TiC(100) prepared in the manner previously described were investigated by successive TPD measurements following a range of D_2O exposures. Figure 1 shows desorption traces for the D_2O molecular ion ($m/q = 20$). Increasing exposures lead to the population of five discernible desorption states labeled in order of decreasing desorption temperature α_1, α_2, α_3, α_4, and β_1. No other desorption features were observed at higher surface temperatures. Four of these states labeled as α saturate with increasing coverage and are related to desorption of species directly adsorbed on the TiC(100) surface. The integrated intensity of D_2O desorption yields ($m/q = 20$), following adsorption at 98 K, versus exposure time is shown in Figure 1B. The linear dependence of integrated intensities for the data of Figure 1A is consistent with a constant (presumably unit) sticking probability below the lowest desorption temperature. We define saturation of the α states to represent the completion of a monolayer, and in turn, the maximum integrated desorption yield from these states (at or above saturation) was used to calculate the D_2O coverage used to describe these experiments.

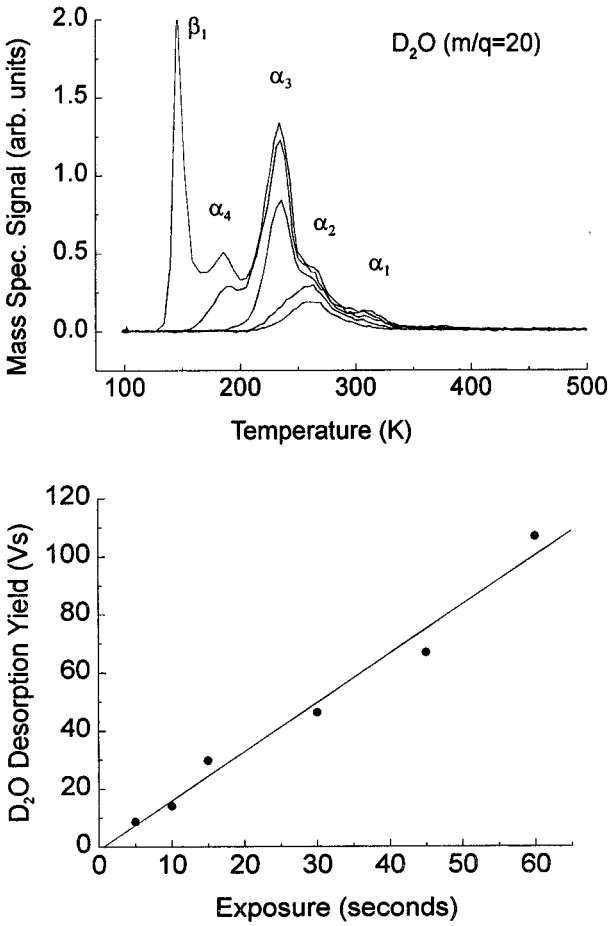

Figure 1. (Upper) D_2O desorption traces ($m/q = 20$) from TiC(100) for increasing exposures of 5, 10, 15, 30 and 45 s through a pinhole doser. The coverages for such exposures in monolayers (see text) are 0.19, 0.30, 0.60, 0.94, and 1.35 ML. The data show successive population of the monolayer and multilayer desorption states. (Lower) The integrated intensities of the D_2O desorption yield indicate a linear uptake of D_2O at 98 K. The linear least-squares regression is also shown.

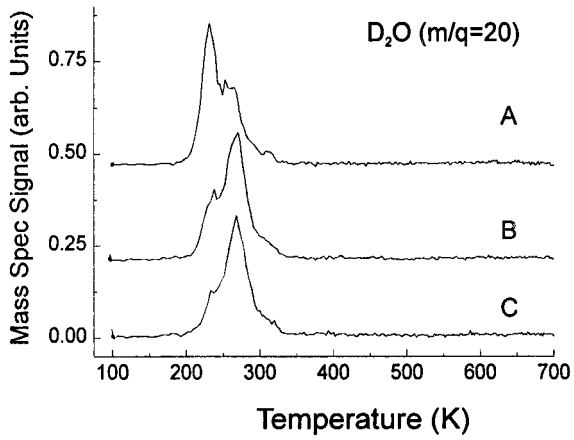

Figure 2. D_2O desorption traces ($m/q = 20$) for 0.60 monolayer coverages (15 s exposures) on freshly sputtered TiC(100) (a) flashed to 1500 K, (b) annealed to 1500 K for 1 min, and (c) annealed to 1500 K for 5 min.

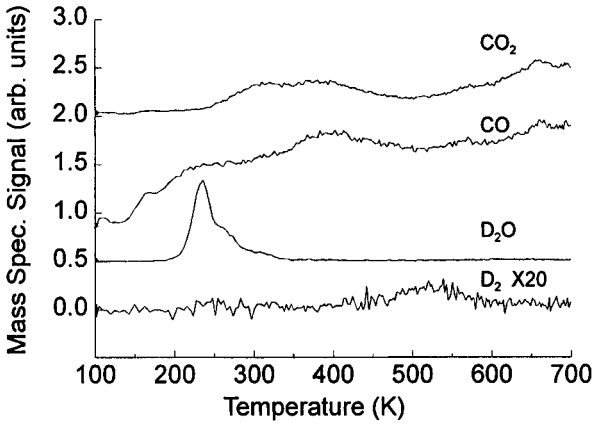

Figure 3. D_2O desorption ($m/q = 20$) and accompanying product evolution of D_2 ($m/q = 4$), CO ($m/q = 28$), and CO_2 ($m/q = 44$) for a 0.60 monolayer coverage (15 s exposure) of D_2O on TiC(100).

In order of decreasing desorption temperature, the first monolayer state, centered at 308 K and labeled α_1, is characterized by a very weak intensity at all coverages; however, it is reproducible and clearly discernible at high mass spectral sensitivities. This state is followed by two other monolayer states, α_2 centered at 263 K and α_3 centered at 233 K, that saturate with increasing coverage. The relative population of the two predominant monolayer states, α_2 and α_3, has been found to be sensitive to the specific nature of surface preparation. Figure 2 displays the desorption of 0.60 ML of D_2O from the TiC(100) prepared by standard sputtering procedures and (a) flashed to 1500 K, (b) annealed to 1500 K for 1 min, and (c) annealed to 1500 K for 5 min. Within experimental error, the total integrated intensity of the D_2O desorption features remains constant, yet a significant shift in intensity from the α_2 state to the α_3 state is observed with increased annealing times. No significant change in the population of the α_1 state is observed, nor are any further spectral changes observed with longer annealing times. With increasing exposures on the well-prepared surface (Figure 1), a state at 188 K labeled α_4 is populated. Together, the α states are attributed to desorption from monolayer species on TiC(100); this dosing system has previously demonstrated monolayer saturation of carbon surfaces under similar exposure conditions at cryogenic temperatures.[16] Finally, the lowest binding energy state at 153 K, labeled β_1, represents desorption from the multilayer. This feature demonstrates the expected peak shape for zeroth-order desorption kinetics, does not saturate with increasing exposure, and is consistent with the multilayer desorption from other surfaces.[17]

Evolution of additional species, directly indicative of a surface reaction, D_2 ($m/q = 4$), CO ($m/q = 28$), and CO_2 ($m/q = 44$), accompanies the desorption of D_2O from the TiC(100) surface. Figure 3 shows these desorption products, together with the molecular water desorption feature for a submonolayer (0.60 ML) D_2O coverage. Desorption traces for CO and CO_2 exhibited reproducible product evolution significantly above background levels across a broad temperature range from 173 to 773 K. While signals for the D_2 evolution were weak, their quality was sufficient to correlate within experimental error the integrated yield near 500 K with the summation of integrated α_1, α_2, and α_3 D_2O desorption intensities. Figure 4 shows a plot of this D_2 product yield versus D_2O coverage. These data were acquired simultaneously to Figure 1.

Vibrational Spectroscopy of D_2O Adsorption States on TiC(100). Figure 5 displays the HREELS spectra of the clean TiC(100) surface (spectrum A), the TiC(100) surface dosed with 25 langmuirs of D_2O at a sample temperature of 144 K (spectrum B), and the identical surface annealed to sequentially higher temperatures and recooled to 144 K (spectra C−F). The intensity of each of the spectra has been multiplied to allow comparison of common spectral features. The multiplication factors are noted in the figure caption. The elastic peak obtained from the clean surface is shown in the leftmost portion of the

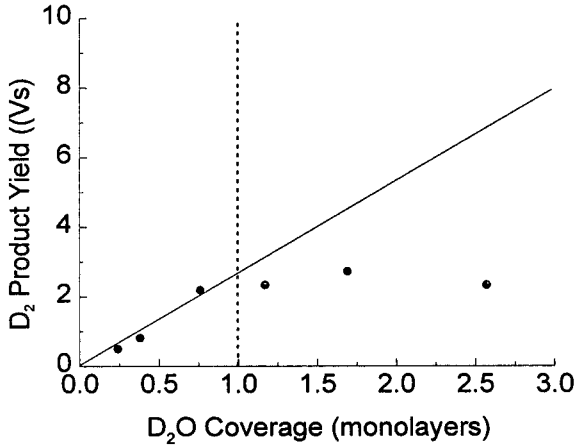

Figure 4. D_2 product yield (integrated intensities) collected simultaneously with the data of Figure 1, showing saturation consistent with the saturation of the monolayer D_2O desorption feature. The solid line is drawn as a guide to indicate a linear increase with coverage.

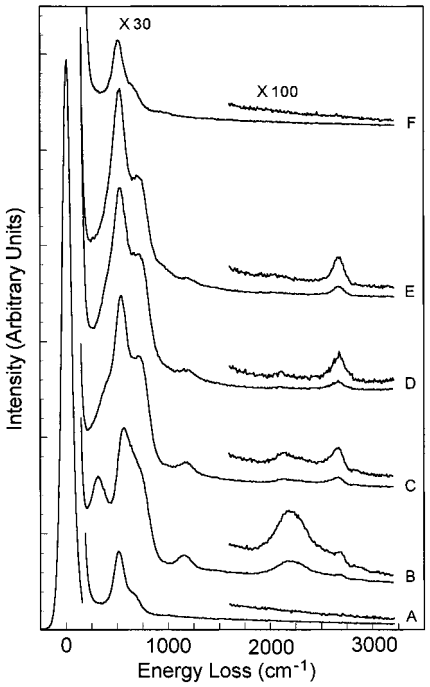

Figure 5. High-resolution electron energy loss spectra of (A) the clean TiC (100) surface, (B) the clean surface after exposure to 25 langmuirs of D_2O at 144 K, and the water-exposed surface following a brief anneal to approximately (C) 173, (D) 203, (E) 228, and (F) 298 K. The spectra collected as a function of annealing temperature were obtained after the sample had been recooled to 144 K. Relative to the clean surface, the scaling factors used in processing these data are (B) 0.99, (C) 1.13, (D) 2.37, (E) 2.17, and (F) 1.06. Relative changes in the intensities of the vibrational features of molecular water and its dissociation products reveal a complex series of reaction and desorption pathways.

figure. The temperature-dependent spectra for the adsorption of H_2O on TiC(100) were also collected to aid in the assignment of spectral features; spectra obtained after annealing to a select number of temperatures are shown in Figure 6. A complete presentation of the spectra for the adsorption of H_2O on TiC(100) will be presented in a separate publication.[18]

In the spectrum of the clean TiC(100) surface (Figure 5A), we find one prominent loss feature at 520 cm^{-1}, due to the Ti−C stretching vibration.[19] In addition, a small shoulder centered at about 640 cm^{-1} is seen to the high-energy side of the Ti−C peak and is attributed to the Ti−O stretch of persistent oxygen species. More extensive studies in this same lab have confirmed

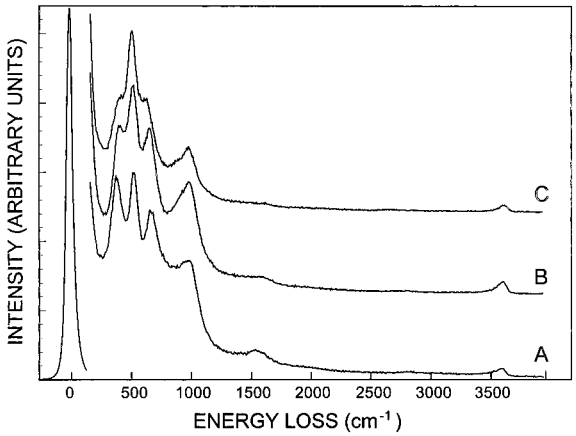

Figure 6. High-resolution electron energy loss spectra of the TiC(100) surface exposed to 2 langmuirs of H_2O and annealed to (A) 153, (B) 193, and (c) 233 K. The spectral assignments of the observed features are listed in Table 1. The scaling factors relative to the spectrum collected from the clean surface are (A) 1.31, (B) 1.27, and (C) 1.36.

by XPS that oxygen comprises ∼5% of the interfacial region probed (∼10 Å in depth).[12] The vibrational data presented here confirm the absence of any other species on the clean surface.

The spectrum obtained after the exposure of the clean TiC(100) surface to 25 langmuirs of D_2O at 144 K (Figure 5b) includes several loss features that result from the vibrations of molecular water and the products of its reaction with the surface. The molecular vibrations of water (D_2O) are the O−D stretching[20,21] and bending[20−22] modes at 2190 and 1150 cm^{-1}, the librational modes[23] of water at 700 and 500 cm^{-1}, the metal−water stretch[24] at 420 cm^{-1}, and a hindered translation[25] of water at 340 cm^{-1}. These assignments are listed in Table 1. It should be noted that second-layer or multilayer water vibrational features were only observed for the series of experiments involving D_2O; the absence of these features in other series of experiments is attributed to slight variations in the lowest attainable surface temperature which fell in the range of multilayer adsorption. Due to the limited resolution of the technique, several of the D_2O features are obviously convoluted with the vibrational features of the clean surface. Experiments performed with H_2O aided in the assignment of these features.

Vibrations due to the dissociation products of D_2O are the non-hydrogen-bonded O−D stretch[20] at 2680 cm^{-1}, the Ti−OD stretch[25] in the range 530−600 cm^{-1}, and a surface hydride stretch at 710 cm^{-1} (Table 1). (The Ti−OD stretch can only be assigned to a spectral region as it is strongly convoluted with the Ti−C stretching vibration of the clean surface.) Again, experiments performed with water lead to the population of analogous O−H, metal−hydroxide, and surface−hydride stretches (Table 1). In particular, the surface hydride stretch is much more clearly resolved at 990 cm^{-1} for the case of H_2O adsorption. The assignment of the 710 cm^{-1} (990 cm^{-1}, H_2O) feature as a surface hydride is also based upon vibrational studies of the adsorption of H_2 on TiC(111) where a similar feature is assigned to the stretch of a hydrogen atom adsorbed in a 3-fold site on the polar metal-terminated face.[26] In analogy, we expect the surface hydride for the TiC(100) to be adsorbed in a multicoordinate site, potentially interacting with both surface carbon and titanium atoms, and thus denote it as (TiC)−D. Although relatively weak in intensity, the C−D stretch at ∼2100 cm^{-1} is also indicative of dissociation upon adsorption.

Following the collection of spectrum B, the D_2O-covered TiC surface was heated to sequentially higher temperatures, holding

TABLE 1: HREELS Assignments (cm^{-1}) for D_2O (H_2O) Adsorption on TiC(100)

	ν(O−H)	ν(C−H)	H_2O scissor	surf. hydride	ν(M−OH_x)	librations	H_2O, hindered translation
2nd layer D_2O, 144 K	2190		1150			700	340
1st layer D_2O, 173 K	2550		1170		420	500	
	(3510)		(1620)		(420)	(680)	
dissociation	2680	2110		710	530−600		
products, 173 K	(3630)	(2750)		(990)	(530−600)		

the sample at the highest temperature for only a few seconds and then cooling to 144 K for the collection of HREELS spectra. Spectra were collected after heating the sample to approximately 153, 163, 173, 203, 228, and 298 K. For clarity, only spectra obtained after annealing to approximately 173, 203, 228, and 298 K are displayed (Figure 5, C−F, respectively). Relative increases and decreases in the different peak intensities of the vibrational features described above were observed with increasing temperatures up to 228 K. In addition to these changes, a small shoulder at 980 cm^{-1} grows between 198 and 228 K and is assigned to a titanium−oxygen double-bond stretch.[27] Upon annealing the surface to 298 K, all the vibrational features associated with molecular water and its dissociation products are absent, and the spectrum closely resembles that of the initial clean TiC(100) surface (Figure 5A). Similar experiments were performed on the H_2O exposed TiC(100) surface. Figure 6 displays the HREELS spectra of this surface following anneals to 153, 193, and 203 K. The details of the changes in these spectra (Figures 5 and 6) associated with sample temperature are discussed below and correlated to the nature of the desorption spectra of D_2O from TiC(100).

Discussion

Together, the results of the thermal desorption experiments with the vibrational spectra measured as a function of temperature can be used to generate a molecularly specific picture of the adsorption, reaction, and desorption pathways of water on TiC(100). We acknowledge that HREELS experiments directly probe only *adsorption states* and TPD experiments directly probe only *desorption states*; however, taken together, the two classes of information can be indirectly related to the surface *reactions* associated with adsorption and desorption. We also acknowledge that some change in the HREELS data may arise from changes in adsorption geometry that would only be fully elucidated by angle-resolved studies. While this may limit the degree of insight gained from the HREELS experiments, the vibrational data together with the TPD data do support the significant observation of low-temperature reactivity on the nonpolar face of this metal carbide. The compound nature of the surface and the dissociation of water result in a number of different surface species involved in a complex series of reaction and desorption processes. In the following sections, we categorize a number of surface processes in terms of surface reactions that occur independent of desorption events and those that accompany specific desorption features seen in the TPD data. The proposed processes have been found to be *consistent* with the data presented and are discussed in order to illustrate the complex nature of reactivity of water with TiC(100).

Surface Reactions. The most significant reaction channel for this system is the decomposition of molecular water upon adsorption at cryogenic temperatures. Evidence for the decomposition of water at these temperatures is clearly seen in the HREELS spectrum, collected after annealing to approximately 173 K (Figure 5C), which contains the vibrational features of a number of dissociation products. These include the O−D stretch of an isolated hydroxide species, the metal−hydroxide stretch, the C−D stretch, and the surface−hydride stretch where hydrogen exists in a multicoordinate site (Table 1). Each of these features is also observed with the corresponding isotopic frequency shift in the spectra collected from the H_2O dosed surface. As evident from the spectral assignments, both the metal and nonmetal components of the surface are involved in this reaction at low temperatures.

An additional reaction observed in these studies involves the decomposition of molecular water that is present in the monolayer at 98 K, as the surface temperature is increased. This reaction pathway involves the dissociation of water in the monolayer regime over the temperature range 173−203 K. In annealing to approximately 203 K, a decrease in intensity of the vibrational features associated with molecular water in the monolayer is correlated with an increase in the intensity of several dissociation products. The intensity of the 1170 cm^{-1} intramolecular deformation mode δ(DOD), assigned by Thiel and Madey as the best basis for the differentiation between molecular water and any or all of its dissociation products,[17] is significantly reduced in this temperature range. (A small intensity for this mode persists to relatively high temperatures; however, this is believed to arise from a minority of surface sites.) As will be discussed, this temperature range also characterizes the desorption of molecularly adsorbed water from the monolayer in the state labeled α_4. However, relative increases in the Ti−OD stretch, the surface−hydride stretch, and most notably the O−D stretch are observed in this temperature range and support the further reaction of molecular water on the TiC(100) as the surface temperature is increased. This assignment is also consistent with our observation of significant D_2O and D_2 desorption in TPD experiments where water is dosed at room temperature (above the highest desorption temperature of any of the water-related species seen in this study). Although the decomposition of water with increasing surface temperature is supported by the vibrational data, these studies do not provide insight into the site specificity of such a process.

The final surface reaction involves the C−D species. Although initially weak in intensity, the C−D stretch is noticeably diminished by annealing to 203 K (Figure 5D). In considering the nature of the compound surface and the adsorption geometry of the surface hydride, we propose that a simple migration (short-range) of the hydrogen atom to a different adsorption geometry may account for this reduction in intensity.

Desorption Pathways. Upon heating the TiC(100) surface dosed with water at cryogenic temperatures, multiple desorption peaks are observed in the TPD spectra for molecular water as well as the TPD spectra of reaction products.

As enumerated in the Results section, the desorption spectra for water (D_2O, $m/q = 20$) contain features in the temperature range from 128 to 298 K (Figure 1). Two features at low temperature are assigned to the desorption of molecular (unreacted) water. At high exposures, the onset of the lowest temperature desorption feature (β_1) occurs at 128 K. This desorption state does not saturate with increasing exposure and exhibits an increasing temperature of desorption maximum with

increasing exposure. These features are characteristic of zeroth-order desorption kinetics and are indicative of the desorption of multilayers of molecular water at this temperature. As described before, the lowest obtainable surface temperature in the HREELS chamber was 144 K. As a result, the vibrational spectrum recorded upon dosing water (Figure 5B) does not include the vibrational signatures of multilayers of ice.[28] A second feature centered at 188 K is assigned to the desorption of molecular water (α_4) from the monolayer of species adsorbed on the TiC(100) surface. Evidence for the desorption of molecularly adsorbed water in this temperature range is seen in the decrease in all of the molecular water features in the monolayer HREELS spectra (Table 1, Figures 5 and 6). The 188 K desorption temperature is within the range of temperatures observed for the desorption of moleculary adsorbed water on the low-index planes of a number of transition metal surfaces.[17] Gaussian peak deconvolution and integration of the TPD data obtained from 1 ML coverage resulted in the α_4 state comprising 20% of the monolayer species, indicating that 20% of the monolayer states result from desorption of molecularly adsorbed water. We speculate that the relatively low concentration of molecularly adsorbed water results from a coverage-dependent adsorption process in which site-dependent dissociative adsorption is limited at high coverages.

The remaining desorption features in the TPD spectra of water and of the other observed products can be associated with a number of surface reactions occurring over a range of surface temperatures. The first of these features involves the desorption of water in the state labeled as α_3, which appears over the range 198−248 K. Deconvolution and integration of α_3 indicates that ∼60% of the monolayer species desorb in this state. We attribute the population of the α_3 state to the recombinative desorption of the surface hydride and surface hydroxide dissociation products. This proposed mechanism is most strongly supported by the substantial decrease in the intensity of the surface hydride over this temperature range which is most clearly seen in the series of spectra involving H_2O (Figure 6B,C). Although this state appears near the low end of the temperature range recognized as characteristic of recombinative desorption,[17] we propose that the surface energetics on this compound surface may differ substantially from that of the widely studied transitional metal surfaces and thus allow bond breaking at these temperatures and subsequent recombination. It is difficult to account for the loss of hydride and hydroxide features in this temperature range through a process not involving a surface reaction.

We propose that the third monolayer desorption feature (α_2) seen in the m/q 20 channel also arises from the recombination of similar decomposition products; however, it arises from different surface sites. In support of this assignment, we note the continued decrease of hydride and hydroxide intensities in this temperature range and that the relative populations of the α_2 and α_3 states are dependent on the method of surface preparation (Figure 2). The TPD results suggest that the two states are site specific, in terms of either the nature of dissociation or recombination pathways at these sites. Although the exact local nature of such sites is not revealed through HREELS and TPD studies, STM images of the TiC(100) surface prepared under similar conditions contain patches of missing atoms.[12] The concentration of such "vacancies" in these images would be consistent with the observed intensity of α_2 (∼10% of the monolayer intensity for the well-prepared surface).

The final desorption feature associated with the desorption of water is the small molecular state ($m/q = 20$) near room temperature (Figure 1, α_1). This small but reproducible state that appears at the highest temperature of all of the water desorption pathways differs from α_2 and α_3 in that the intensity of this channel is not appreciably altered by differing surface preparations. In light of the persistence of a surface species involving oxygen to near room temperature, as seen by XPS,[18] it is possible that the pathway leading to the population of this TPD state may be mediated by the specific sites created by the reaction of water with the TiC surface. At low water coverages, a similar desorption feature is observed at ∼323 K for water desorption from single-crystal TiO_2.[29] Alternatively, we believe that this channel may be associated with the disproportionation reaction of surface hydroxides. This reaction mechanism for the production of gas-phase, molecular water has been observed for the desorption of water from Fe(100)[30] and Ni(110).[31] From the data available, we are unable to conclude the exact role of surface oxygen or the exact pathway leading to desorption at this temperature; however, we note that this desorption channel arises from a relatively small fraction of the monolayer species (∼10%).

Apart from the desorption of molecular water, two carbon-containing species are observed. As indicated in Figure 3, the desorption of carbon monoxide and carbon dioxide is observed over a broad range of temperatures. This desorption behavior and the absence of carbon−oxygen features in the HREELS data are consistent with the desorption of relatively short-lived surface species involving surface carbon and oxygen. This behavior is also consistent with previous reports of the spontaneous evolution of CO_x species from TiC surfaces upon exposure to oxygen.[6,27] In HREELS studies of the adsorption of O_2 on TiC(100) at cryogenic temperatures, no features associated with carbonyl species are observed and indicate that CO or CO_2 is evolved from the surface immediately upon the dissociation of oxygen. It is reasonable that a similar reaction pathway occurs for carbon−oxygen species produced by the dissociation of water or disproportionation of adsorbed hydroxyls on the TiC surface. While the observation of carbon-containing species in TPD spectra further illustrates the complex nature of the reactions that occur upon exposure of TiC(100) to water, the broad nature of desorption features limits the insight into the specific pathways leading to such desorption.

The final desorption pathway observed from the TiC(100) surface exposed to deuterated water involves the production of D_2 (Figure 3). The desorption behavior of this product is unique from the others in that a single isolated desorption peak is observed at relatively high temperatures (∼500 K). As shown in the plot of D_2 integrated desorption intensity versus D_2O coverage (Figure 4), the desorption of D_2 can be correlated to the monolayer coverage regime, but not to a specific desorption state of molecular water (α_1, α_2, or α_3). It is noteworthy that the same experiments, in which shorter anneal times lead to a greater population of the α_2 D_2O desorption state, also lead to a greater production of D_2 at the same high temperatures. We do not believe that the production of D_2 is directly related to the species leading specifically to the α_2 desorption state, but rather is related to the existence of surface defects. Carbon vacancies on TiC(100) have been previously identified by Aono and co-workers using impact-collision ion-scattering spectroscopy (ICISS)[32] and by our group with STM. However, we do not have exact knowledge of the local structure of these sites and are therefore unable to identify the specific pathway to the production of D_2. Although potentially participating in the

production of D_2, we believe that such sites do not dominate the reactivity of water on TiC(100) as described in the previous sections.

Conclusions

The interaction of water with the nonpolar face of TiC at cryogenic temperatures has been probed by temperature-programmed desorption and high-resolution electron energy loss spectroscopy. Together, these molecularly specific probes of the adsorption and desorption pathways reveal a complex series of reactions occurring on this metal−carbide surface. From these data, a number of important general conclusions can be drawn about the interaction of water with this face of titanium carbide. (i) Water adsorbs both molecularly and dissociatively in the monolayer regime when exposed to TiC(100) at cryogenic temperatures. (ii) Further surface reaction of water competes with desorption with increasing surface temperature. (iii) Both Ti and C atoms at the surface contribute to the observed reactivity and the production of an array of surface species. (iv) CO, CO_2, and D_2 are observed as minority desorption species and demonstrate the removal of carbon from the TiC surface and the potential activity of carbon vacancies known to exist within this and other metal carbides. Finally, this study clearly demonstrates the significant changes that can occur at one of the least reactive faces of TiC when exposed to a common atmospheric species, water, and highlights the important role adsorbates such as water may play in determining the tribological properties of this hard coating material.

Acknowledgment. This work has been supported by the AFOSR under Contract F49620-97-0029. Partial support has also been provided through The Aerospace Corporation IR&D program funded by the Space and Missile Systems Center (SMC) of the USAF under Contract F04701-93-C-0094.

References and Notes

(1) For example, see: Kawata, K. *Surf. Coat. Technol.* **1992**, *54/55*, 604.

(2) Boving, H. J.; Hintermann, H. E. *Tribol. Int.* **1990**, *23*, 129 and references therein.

(3) Toth, L. E. *Transition Metal Carbides and Nitrides*; Academic Press: New York, 1991.

(4) Oshima, C.; Aono, M.; Tanaka, T.; Kawai, S.; Zaima, S.; Shibata, Y. *Surf. Sci.* **1981**, *102*, 312.

(5) Edamoto, K.; Anazawa, T.; Miyazaki, E.; Kato, H.; Otani, S. *Surf. Sci.* **1993**, *287/288*, 667.

(6) Souda, R.; Aizawa, T.; Otani, S.; Ishizawa, Y. Oshina, C. *Surf. Sci.* **1991**, *256*, 19.

(7) Jansen, S. A.; Hoffmann, R. *Surf. Sci.* **1988**, *197*, 474.

(8) Didziulis, S. V.; Lince, J. R.; Stewart, T. B.; Eklund, E. A. *Inorg. Chem.* **1994,** *33*, 1979.

(9) Johansson, L. I. *Surf. Sci. Rep.* **1995**, *21*, 177.

(10) Otani, S.; Honma, S.; Tanaka T.; Ishizawa, Y. *J. Cryst. Growth* **1983**, *61*, 1.

(11) Perry, S. S.; Merrill, P. B. *Surf. Sci.* **1997**, *383*, 268.

(12) Frantz, P.; Didziulis, S. V.; Merrill, P. B.; Perry, S. S. *Tribol. Lett.* **1998**, *4*, 141.

(13) Hatch, S. R. Ph.D. Dissertation, University of Texas, 1990.

(14) Yates, Jr., J. T. *J. Vacuum Sci. Technol. A* **1987**, *5*, 1.

(15) Didziulis, S. V.; Fleischauer, P. D. *Langmuir* **1990**, *6*, 621.

(16) Initial calibrations of the dosing system utilized D_2O adsorption on amorphous carbon (a:C−H_x). At cryogenic temperatures, the exposures necessary to obtain multilayer adsorption on this inert surface are consistent with those for TiC(100).

(17) Thiel, P. A.; Madey, T. E. *Surf. Sci. Rep.* **1987**, *7*, 211.

(18) Didziulis, S. V.; Frantz, P.; Merrill, P. B.; Imaduddin, S.; Elbjeirami, O.; Perry, S. S., to be published.

(19) Chen, J. G.; DeVries, B. D.; Fruhberger, B.; Kim, C. M.; Liu, Z.-M. *J. Vauum Sci. Technol.* **1995**, *13*, 1600.

(20) Olle, L.; Salmeron, M.; Baro, A. M. *J. Vacuum Sci. Technol. A* **1985**, *3*, 1866.

(21) Wu, M.-C.; Estrada, C. A.; Goodman, D. W. *Phys. Rev. Lett.* **1991**, *67*, 2910.

(22) Brousseau, R.; Brustein, M. R.; Ellis, T. H. *Surf. Sci.* **1993**, *280*, 23.

(23) Thiel, P. A.; DePaola, R. A.; Hoffmann, F. M. *J. Phys. Chem.* **1984**, *80*, 5326.

(24) Phelps, R. B.; Kesmold, L. L.; Kelley, R. J. *Surf. Sci.* **1995**, *340*, 134.

(25) A range of expected frequencies is generated from a careful consideration of analogous systems described in the review article by Thiel and Madey (ref 17).

(26) Oshima, C.; Aono, M.; Otani, S.; Ishizawa, Y. *Solid State Commun.* **1983**, *48*, 911.

(27) Frantz, P.; Didziulis, S. V. *Surf. Sci.*, in press.

(28) Hardin, A. H.; Harvey, K. B. *Spectrochim. Acta* **1973,** *A29*, 1139.

(29) Henderson, M. A. *Surf. Sci.* **1994**, *319*, 315.

(30) Barb, A. M.; Erley, W. *J. Vacuum Sci. Technol.* **1982**, *20*, 580.

(31) Benndorf, C.; Nöbl, C.; Madey, T. E. *Surf. Sci.* **1984**, *138*, 292.

(32) Aono, M.; Hou, Y.; Souda, R.; Oshima, C.; Otani, S.; Ishizawa, Y. *Phys. Rev. Lett.* **1983**, *50*, 1293.